Turkish J. Eng. Env. Sci.
30 (2006) , 145 – 155.

Importance of Buoyancy and Chemistry Modelling in Steady RANS Simulations of Well-Ventilated Tunnel Fires

Karim VAN MAELE, Bart MERCI
Ghent University – UGent, Department of Flow, Heat and Combustion Mechanics
Sint-Pietersnieuwstraat 41, B-9000 Ghent-BELGIUM
e-mail: Karim.VanMaele@UGent.be

Received 01.06.2006

Abstract

Numerical CFD simulation results are presented for well-ventilated fires in horizontal tunnels. Simulations are performed in the framework of steady Reynolds-Averaged Navier-Stokes modelling. As a turbulence model, a 'realisable' k-ε model is applied. Both the simple and generalised gradient diffusion hypotheses are compared as models for the buoyancy production of turbulent kinetic energy. Within the framework of the conserved scalar approach (with the mixture fraction as conserved scalar), with pre-assumed β-PDF modelling for the turbulence-chemistry interaction, 2 combustion models are compared as well: a steady laminar flamelet model with a constant strain rate and the full chemical equilibrium model. The simple and the generalised gradient diffusion approach for buoyancy modelling give similar results for the global flow field. However, large differences are visible in the region of smoke reversal. This is important with respect to the prediction of the critical ventilation velocity, an important design parameter for tunnels that should be correctly predicted by numerical simulations. Details of the chemistry model have only a small influence on the prediction of the global flow field. Even for the quantitative determination of the critical ventilation velocity, the differences between the combustion models considered are small. The realisable k-ε model, with the generalised gradient diffusion hypothesis for the buoyancy source term, gives satisfactory results for the prediction of the critical velocity, with both chemistry models applied.

Key words: Tunnel fire, Critical ventilation velocity, Buoyancy modelling, Chemistry modelling, Steady simulations.

Introduction

For improvement of the fire safety of all kinds of infrastructures, numerical predictions with computational fluid dynamics (CFD) are becoming an important and widespread tool. Since CFD, or field modelling, is based on the solution of the fundamental conservation laws of mass, momentum, energy, and chemical species, it has the potential of providing detailed and reliable information on the behaviour of a fire and the movement of smoke in complex geometries. However, it is impossible to obtain first-principle solutions (Direct Numerical Simulations or DNS) of these equations because of the broad range of time and length scales present in fire-induced flows, which are due to turbulence and chemical reactions occurring in the flow-field. For practical fire simulations, this would require a tremendous amount of computer power and memory, which is intractable with present-day computers. Therefore, some filtering of the governing equations has to be applied. Based on the filtering method, 2 major classes of field models can be distinguished: Reynolds-Averaged Navier-Stokes (RANS) simulations and Large Eddy Simulations (LES). With LES, the large-scale motions of the flow are resolved and great accuracy of the predicted flow field can be obtained. With the RANS approach, all turbulent motions are filtered out by ensemble-averaging of the governing equations and the effect of turbulence on the mean

flow field is incorporated by a turbulence model. Although LES is thought of as the next step in fire modelling (Novozhilov, 2001), it is still not applicable for practical simulations, due to the limited capacity of present-day computers. Nonetheless, performing time-accurate simulations with LES (e.g. Fire Dynamics Simulator of NIST, http://fire.nist.gov/fds) is a promising practice, provided that the models are applied correctly. However, in the authors opinion, research on steady-state RANS simulations must not be abandoned at the moment. One reason is that correctly performed LES simulations must be executed on a much finer computational mesh than what is needed for steady RANS simulations. As such, at least 1 or 2 orders of magnitude in time are gained in steady RANS simulations. Within this framework, the best models possible must be applied and there is still room for improvement in different aspects. In this paper, the focus is primarily on the turbulence model, and in particular on the modelling of the effect of buoyancy. The effect of the chemistry model is examined within the framework of the conserved scalar. The mixture fraction acts as the conserved scalar. The pre-assumed β-PDF (Probability Density Function) approach is applied to incorporate interaction between turbulence and combustion. For the chemistry, both the full chemical equilibrium model (infinitely fast reactions) and a steady laminar flamelet model, with a single strain rate, are considered.

In Van Maele and Merci (2006), the focus is on the application of the standard and realisable k-ε turbulence model to thermal plume flows: the buoyant axisymmetric turbulent plume and 2-dimensional buoyant turbulent wall plume. The major conclusion is that the realisable k-ε model, in combination with the generalised gradient diffusion hypothesis for modelling of the buoyancy production term, has good potential for use in fire-driven flows. In the present work, we concentrate on the more complex case of the ventilated tunnel fire in order to make a further verification of the applicability of the modified realisable k-ε model. Several variants for the term representing the buoyant production of k are compared for the case of a fire in a well-ventilated horizontal tunnel. Where the buoyant plumes in Van Maele and Merci (2006) are flows without combustion, the present case involves chemical reactions, which makes the case more complex. In a previous work (Merci and Van Maele, 2005), results are presented of simulations of a 30 kW fire in the same tunnel as considered here, obtained with the standard k-ε model. These results were not satisfactory as they were not realistic for the ventilation speed considered there; in contrast to the experiments with the same ventilation velocity, the flame was pushed against the floor of the tunnel and no rising plume was observed. Therefore, here we concentrate on the realisable k-ε model, which produces more realistic flow-fields.

The structure of the paper is as follows. First, the tunnel test case is briefly described. Afterwards, the sub-model for turbulence applied in the simulations, along with its modifications for buoyancy driven flows, is presented. Next, the chemistry models applied are given. After providing some details about the numerical set-up of the simulations, results are presented and followed by a discussion. At the end, some conclusions are drawn.

Test Case Description

The tunnel fires considered in the present paper have been studied experimentally by Wu and Bakar (2000). They carried out experiments on 5 model tunnels with different internal cross-sections. Here, we consider 2 cross-sections only: the tunnel with a square cross-sectional area with height equal to width of H = W = 0.25 m ('tunnel B') and the tunnel with a rectangular shape with the same height of H = 0.25 m, but a width of W = 0.50 m ('tunnel C'). The acronyms 'B' and 'C' are adopted from Wu and Bakar (2000). A circular porous bed burner (diameter: D = 106 mm), with its top surface set flush with the tunnel floor, is placed centrally at the bottom of the cross-section, with its centre point 6.21 m from the tunnel inlet. The tunnel outlet is 8.71 m from the burner centre point. Propane gas is used as fuel. In the experiments, different thermal powers, ranging from 1.5 to 30 kW were applied by adjusting the propane mass flow rate. Here, we consider the 15 kW fire only. The ventilation flow in the experiments was driven by compressed air, which passed through an orifice plate to determine the volumetric flow of the ventilation air.

In the case of a tunnel fire, horizontal ventilation can be used to create a safe, smokeless upstream route for use by fire fighters and for the evacuation of victims. However, when the power of this ventilation is insufficient, "back layering" of the smoke can occur, i.e. smoke can flow in the opposite direction of the ventilation air. This poses a considerable threat

for fire fighters and occupants of vehicles caught upstream of the fire because of the heat radiated from the hot smoke layer and the presence of toxic gases. Therefore, the critical velocity, i.e. the ventilation velocity for which there is no back layering, is an important design parameter for tunnels that should be correctly predicted by CFD simulations. For the experiments carried out by Wu and Bakar (2000), the critical velocity is measured for all configurations.

Turbulence modelling

In this work, we apply the k-ε model developed by Shih et al. (1995), which was originally formulated for constant density flows. However, the flows generated by a fire are mainly driven by buoyancy; the driving forces for the flow are the density differences in the field generated by the release of heat in the flames. In order to obtain reliable flow field predictions, the main effect of buoyancy on turbulence (increase of the turbulence level in unstable stratified situations and suppression in stable stratified regions) has to be incorporated in the turbulence model. This is accomplished by including a buoyancy source term in the transport equation, for both the turbulent kinetic energy and turbulent dissipation rate. In the model applied here, k and ε are determined from the steady transport equations:

$$\frac{\partial}{\partial x_j}\left(\bar{\rho}k\widetilde{u_j}\right) = \frac{\partial}{\partial x_j}\left[\left(\mu + \frac{\mu_t}{\sigma_k}\right)\frac{\partial k}{\partial x_j}\right] + P + G - \bar{\rho}\varepsilon \tag{1}$$

$$\begin{aligned}\frac{\partial}{\partial x_j}\left(\bar{\rho}\varepsilon\widetilde{u_j}\right) &= \frac{\partial}{\partial x_j}\left[\left(\mu + \frac{\mu_t}{\sigma_\varepsilon}\right)\frac{\partial \varepsilon}{\partial x_j}\right] \\ &\quad + \bar{\rho}C_1 S\varepsilon - \bar{\rho}C_2\frac{\varepsilon^2}{k+\sqrt{\upsilon\varepsilon}} + S_{\varepsilon B},\end{aligned} \tag{2}$$

with P the production of turbulent kinetic energy due to turbulent stresses (mainly shear) and mean flow gradients, G the production of k due to the effect of buoyancy, and $S_{\varepsilon B}$ the buoyancy source term in the equation for the turbulent dissipation rate. The expressions for G and $S_{\varepsilon B}$ are given below. An important difference with the ε-equation of the standard k-ε model is that the shear-related production term is no longer the production of turbulent kinetic energy P divided by the turbulent time scale k/ε. This resolves the well-known plane jet-round jet anomaly problem of the standard k-ε model. More details about the derivation of this ε-equation can be found in the work of Shih et al. (1995). The model constants have the values $C_2 = 1.9, \sigma_k = 1.0, \sigma_\varepsilon = 1.2$.

The model of Shih et al. (1995) is called 'realisable' because it satisfies certain mathematical laws the turbulent stresses have to obey; the turbulent normal stresses do not become positive and the Schwarz inequality for the turbulent shear stresses is fulfilled. When these laws are violated, it means that the turbulent stresses predicted by the turbulence model are not physically possible. As with the standard k-ε, the turbulent stresses are calculated with a first order constitutive law:

$$\begin{aligned}\tau_{ij}^t &= -\bar{\rho}\widetilde{u_i''u_j''} = -2/3\delta_{ij}\bar{\rho}k + 2\mu_t S_{ij}, S_{ij} \\ &= \frac{1}{2}\left(\frac{\partial\widetilde{u_i}}{\partial x_j} + \frac{\partial\widetilde{u_j}}{\partial x_i}\right) - \frac{1}{3}\frac{\partial\widetilde{u_l}}{\partial x_l}\delta_{ij},\end{aligned} \tag{3}$$

with S_{ij} the strain rate tensor and the turbulent viscosity calculated as

$$\mu_t = \bar{\rho}C_\mu k^2/\varepsilon. \tag{4}$$

In the standard k-ε model, the model parameter C_μ has the constant value 0.09. In the realisable k-ε model, however, this parameter is made sensitive to the local mean strain and rotation of the flow field to ensure the realisability of the turbulence model. More details about the calculation of C_μ can be found in Shih et al. (1995).

As noted before, fire-generated flows are driven by buoyancy and this has a large influence on the production/destruction of turbulent kinetic energy. This effect is included with the buoyancy source terms G and $S_{\varepsilon B}$. When the transport equation for k is derived form the Favre-averaged low Mach number equations, the buoyancy source term G appears as:

$$G = -\overline{u_j''}\left(\frac{\partial p}{\partial x_j} + \rho_0 g_j\right) = \frac{\overline{\rho' u_j'}}{\bar{\rho}}\left(\frac{\partial p}{\partial x_j} + \rho_0 g_j\right). \tag{5}$$

If the reference density$\rho_0$is chosen such that everywhere $|\partial p/\partial x_j| \ll \rho_0 g_j$, and if the ('Boussinesq') approximation$\bar{\rho} \approx \rho_0$ is made, the buoyancy term becomes $G = \overline{\rho' u_j'} g_j$. In the reference frame applied (see nomenclature section), the buoyancy

source term can be written as $G = -\overline{\rho' v'} g$(with g= 9.81 m/s^2). Two different approaches are applied to model the unknown density-velocity correlation $\overline{\rho' v'}$. In the first approach, the simple gradient diffusion hypothesis (SGDH) is used and the buoyancy term is expressed as:

$$G = -g \frac{\mu_t}{\sigma_t} \frac{1}{\bar{\rho}} \frac{\partial \bar{\rho}}{\partial y}, \tag{6}$$

with the turbulent Prandtl number $\sigma_t = 0.85$.

In the second approach, the correlation $\overline{\rho' v'}$ is modelled using the generalised gradient diffusion hypothesis (GGDH) of Daly and Harlow (1970), here written in terms of density gradients:

$$\overline{\rho' v'} = -c_t \frac{k}{\varepsilon} \left(\overline{u' v'} \frac{\partial \bar{\rho}}{\partial x} + \overline{v' v'} \frac{\partial \bar{\rho}}{\partial y} + \overline{v' w'} \frac{\partial \bar{\rho}}{\partial z} \right). \tag{7}$$

where $c_t = 1.5 C_\mu / \sigma_t$. Ince and Launder (1989) were probably the first to use the GGDH, which afterwards was used by several other authors (Yan and Holmstedt, 1999; Worthy et al., 2001; Brescianini and Delichatsios, 2003). Since k-ε turbulence models are not suited for predicting the normal turbulent stresses accurately, we suggest replacing this stress in Eq. (7) by the turbulent kinetic energy k. For the buoyant plume, this is a very good assumption (Van Maele and Merci, 2006). The resulting model for G can be written as follows, where expression (4) is used to replace C_μ,

$$G = -g \frac{3}{2} \frac{\mu_t}{\bar{\rho} k \sigma_t} \left(\overline{u' v'} \frac{\partial \bar{\rho}}{\partial x} + k \frac{\partial \bar{\rho}}{\partial y} + \overline{v' w'} \frac{\partial \bar{\rho}}{\partial z} \right). \tag{8}$$

The main difference with expression (6) is the inclusion of transversal density gradients into the buoyancy production term, making that G have a stronger effect on the numerical results (Van Maele and Merci, 2006).

In addition to the buoyancy production/destruction term in the k-equation, there is also a buoyancy source term in the equation for the turbulent dissipation rate ($C_{1\varepsilon} = 1.44, C_{3\varepsilon} = 0.8$); for more details see Van Maele and Merci (2006):

$$S_{\varepsilon B} = C_{1\varepsilon} (1 - C_{3\varepsilon}) \frac{\varepsilon}{k} G. \tag{9}$$

Chemistry model

Inclusion of the combustion process in the simulations requires an additional model. Here, the conserved scalar approach is followed, with the mixture fraction as conserved scalar. Interaction between turbulence and chemistry is modelled with the pre-assumed β-PDF (Probability Density Function) model. This has the advantage that the PDF can adopt very different types of shapes, depending on the values of mean mixture fraction and mixture fraction variance, thus representing different types of mixing regimes. The standard steady transport equations for the mean mixture fraction ($\tilde{\xi}$) and its variance ($\widetilde{\xi''^2}$) are solved:

$$\frac{\partial}{\partial x_j} \left(\bar{\rho} \widetilde{u_j} \tilde{\xi} \right) = \frac{\partial}{\partial x_j} \left(\frac{\mu_t}{\sigma_\xi} \frac{\partial \tilde{\xi}}{\partial x_j} \right) \tag{10}$$

$$\begin{aligned} \frac{\partial}{\partial x_j} \left(\bar{\rho} \widetilde{u_j} \widetilde{\xi''^2} \right) &= \frac{\partial}{\partial x_j} \left(\frac{\mu_t}{\sigma_g} \frac{\partial \widetilde{\xi''^2}}{\partial x_j} \right) \\ &\quad + C_g \mu_t \frac{\partial \tilde{\xi}}{\partial x_j} \frac{\partial \tilde{\xi}}{\partial x_j} - C_d \bar{\rho} \frac{\varepsilon}{k} \widetilde{\xi''^2}, \end{aligned} \tag{11}$$

with the model constants $\sigma_\xi = \sigma_g = 0.85, C_g = 2.86, C_d = 2.0$.

The relation between the mixture fraction and the species mass fraction, temperature and density, is established through the chemistry model. The first model applied is a steady laminar flamelet model (SLFM), based on the C_1 skeletal scheme of Correa (1993). This mechanism contains 16 species (CH_4, O_2, H_2O, CO_2, CO, OH, CH_2O, H_2, HO_2, H_2O_2, O, H, HCO, CH_3, CH_3O and N_2) and 41 reactions. Since propane is not included in this chemical mechanism, the fuel in the simulations is replaced by methane and the inlet mass flow rate at the burner is adjusted in order to keep the fire load constant. A constant strain rate (a = 100 s^{-1}) is applied for the construction of the laminar flamelet table. The use of a single strain rate value, rather than a library of flamelets, is a simplification. Extension of this is considered as future work.

In order to assess the impact of the chemistry model on the flow field results, a full chemical equilibrium model (FCE) with 26 species (CH_4, N_2, O_2, C_2H_6, CO, CO_2, H_2, H_2O, NH_3, solid C, NO, NO_2, OH, HO_2, N_2O, O, HONO, H, H_2O_2, HNO, N, HCN, CH_2O, HCOOH, HNCO, C_2H_4) is also used. With the commercial CFD Fluent code version 6.2, we

were unable to apply the 16 species of Correa's mechanism in combination with the full chemical equilibrium model. As with the flamelet model, it is assumed that the fuel is methane instead of propane. Again, the mass flow-rate is adjusted to get the correct thermal load in the tunnel.

Radiation model

The fire source thermal power is chosen to be large enough for the flow field to become more or less independent of the exact value of the fire load (Wu and Bakar, 2000). As a consequence, it is of less importance to include radiation modelling, since the radiative losses are, to a certain extent, similar to the application of a reduced fire load. Obviously, the absolute temperatures will be too high. Since only the critical ventilation velocity is studied in a quantitative manner and otherwise qualitative behaviour is concerned here, the modelling of radiation is omitted.

Numerical Aspects

The governing equations are solved with the commercial CFD package, Fluent 6.2. Second-order upwinding is used for the convective terms in the momentum, energy, and turbulence equations. The SIMPLE algorithm is used for the coupling between velocity and pressure.

The tunnel fire simulations are performed on a 3-dimensional grid. For both cross-sectional geometries, only half of the tunnel is simulated due to the symmetry of the flow in the tunnel. The cross-sectional geometry of the computational mesh is the same as in the experiments, but the tunnel is made slightly shorter in the numerical simulations, as was done in Wu and Bakar (2000); for tunnel B it starts 5 m upstream of the burner and ends 3 m downstream of the burner, for tunnel C, it starts 3 m upstream of the burner and ends 3 m downstream of the burner. The mesh for tunnel B consists of 108 x 28 x 14 cells. The 108 cells in the longitudinal direction are distributed as follows: 34 cells upstream of the burner (with the smallest cell size equal to 1 cm at the burner front-end and stretching toward the inlet), 10 equidistant cells over the burner surface, and 64 cells downstream of the burner (again, the smallest cell size equal to 1 cm at the burner and stretching toward the outlet boundary). The cells in the cross-sectional direction are square (size equal to 9 mm). The mesh for tunnel C consists of 78 x 28 x 26 cells. The distribution of the cells in the longitudinal direction is as follows: 34 cells upstream and downstream of the burner and 10 equidistant cells over the burner front. Again, the cells are stretched towards the inlet and outlet of the tunnel. At the tunnel inlet boundary, uniform values are imposed for the velocity components, turbulent kinetic energy and dissipation rate, mean mixture fraction (equal to zero: pure air), and mixture fraction variance (also equal to zero: no composition fluctuations), while pressure is extrapolated from the flow field. Another approach is the application of separately calculated, fully developed turbulent profiles. This has, however, no influence on the results (not shown). At the burner inlet, the same procedure is applied (mixture fraction equal to 1: pure fuel). The turbulence intensity has been set to 10% and the turbulent length scale equal to $l_m = c_\mu^{0.75} k^{1.5}/\varepsilon = D/15$, with D the burner diameter (Merci et al., 2002). In the simulations, the circular burner has been replaced by a square shape with the same surface area, as was done in Wu and Bakar (2000). At the tunnel outlet boundary, atmospheric pressure is imposed and zero derivatives in the longitudinal direction are applied for all other quantities.

Results and Discussion

First, results are presented for tunnel B with a thermal load of 15 kW. All results are obtained with the realisable k-ε model. To begin with, we compare the results obtained with the 2 models for buoyancy (SGDH and GGDH). In Figure 1, both temperature (K) contours and velocity vectors are presented in the symmetry plane of the tunnel, in the vicinity of the burner. The steady laminar flamelet model is applied to incorporate the combustion process. Results are shown for a ventilation velocity of 0.5 m/s.

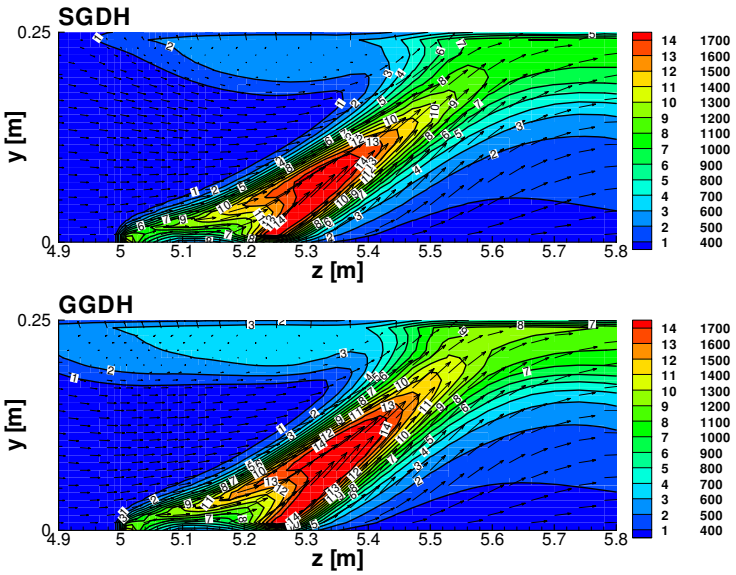

Figure 1. Temperature contours and velocity vectors in the symmetry plane (tunnel B). Comparison of SGDH and GGDH buoyancy model. Chemistry: SLFM. U_{in} = 0.5 m/s.

Wu and Bakar (2000) presented measured temperature contours for the 15 kW fire in tunnel B with the critical ventilation velocity at the tunnel inlet. Since the temperatures in our simulations are too high, because radiation has been neglected, only quantitative comparisons are made for the critical ventilation velocity. Table 1 gives the critical ventilation velocity for this tunnel fire. In the experimental study by Wu and Bakar (2000), it was found that the critical ventilation velocity for the 15 kW fire in tunnel B was 0.6 m/s. It is clear from Figure 1 that with the SGDH model the critical velocity is substantially under-predicted; with this approach it follows that there is no reversal of the hot smoke layer upstream from the leading edge of the burner with U_{in} = 0.5 m/s, i.e. this is the predicted critical ventilation velocity. The realisable k-ε model in combination with the GGDH approach is more accurate since it predicts back layering with the applied ventilation velocity of 0.5 m/s. The critical velocity was found to be U_{in} = 0.54 m/s. It is interesting to note in Figure 1 that, except from the zone with the smoke reversal, the global flow field obtained with the SGDH and GGDH approach is nearly the same. An explanation for this is that the production of turbulent kinetic energy is dominated by shear rather than buoyancy. As a consequence, outside the region where buoyancy is far more important than shear, the 2 variants of the buoyancy production term have the same impact on the results. In the impingement zone of the plume, the temperatures obtained with the GGDH approach are higher than with the SGDH approach, which is explained by the larger amount of hot gases that travels upstream, due to stronger buoyancy effects, with the GGDH model.

Table 1. Comparison of the experimentally determined critical ventilation velocities and the critical ventilation velocities predicted by the CFD simulations.

Case	Measured	SGDH-SLFM	GGDH-SLFM	SGDH-FCE	GGDH-FCE
B – 15 kW	0.60 m/s	0.50 m/s	0.54 m/s	0.50 m/s	0.54 m/s
C – 15 kW	0.60 m/s	0.57 m/s	0.60 m/s	0.57 m/s	0.60 m/s

In Figure 2, we present the results of the 15 kW fire in tunnel B with the predicted critical ventilation velocity of $U_{in} = 0.54$ m/s for the GGDH model. Although this is still lower than the experimental critical velocity of 0.6 m/s, it is more accurate than the critical velocity obtained with the classical SGDH approach (see Table 1). In addition to the flamelet model, the full chemical equilibrium (infinitely fast reactions) is applied. Both models predict the same critical velocity and there is practically no difference in the flow fields obtained. However, there is a slight difference in the temperature contours; the highest temperatures in the flame obtained with the equilibrium model are lower than those in the flame obtained with the flamelet model. This has, however, no effect on the amount of hot smoke that travels opposite to the external ventilation because the temperatures in the impingement region are equal for both models. The global flow field is very similar and the tilting of the flame due to the ventilation is roughly the same. Since chemistry is fast, compared to the turbulent mixing, the detail of the chemistry model is not crucial in the simulation results. Since the major mechanism is definitely non-premixed turbulent combustion, it is no surprise that the chemistry effects cannot strongly affect the flow field dynamics (turbulent mixing). Temperatures (or densities) that result from the applied chemistry model are important input parameters for the buoyancy part of the turbulence model, and as such, quantitatively affect the numerical results.

A further illustration of the 2 combustion models is given in Figures 3 and 4. Contour plots are shown for the mass-fraction CO_2 (Figure 3) and CO (Figure 4) present in the flow-field. The results are given for the 15 kW fire in tunnel B (with a ventilation velocity of 0.54 m/s) with both the flamelet and chemical equilibrium model applied.

In the experiments, no species mass-fractions were measured, so only qualitative statements can be made on the differences between both chemistry models. For species CO_2, the shape of the chemical contours is very similar to the shape of the temperature contours. The chemical equilibrium model predicts lower values of CO_2 in the flame than the flamelet model. This is consistent with the lower temperatures, compared to the flamelet model, in the same region predicted by the equilibrium model. For species CO, the shape of the contours obtained with both chemical models is very similar, but there is a large difference in the predicted values. The peak values predicted by the equilibrium model are 5 times larger than the peak values obtained with the flamelet model. This again indicates a much stronger tendency toward incomplete combustion (despite imposing full equilibrium). This is due to the inclusion of other species in the equilibrium model that are not included in the SLFM. As noted before, it was impossible in Fluent 6.2 to apply the full chemical equilibrium model with the same species as used in the steady laminar flamelet model.

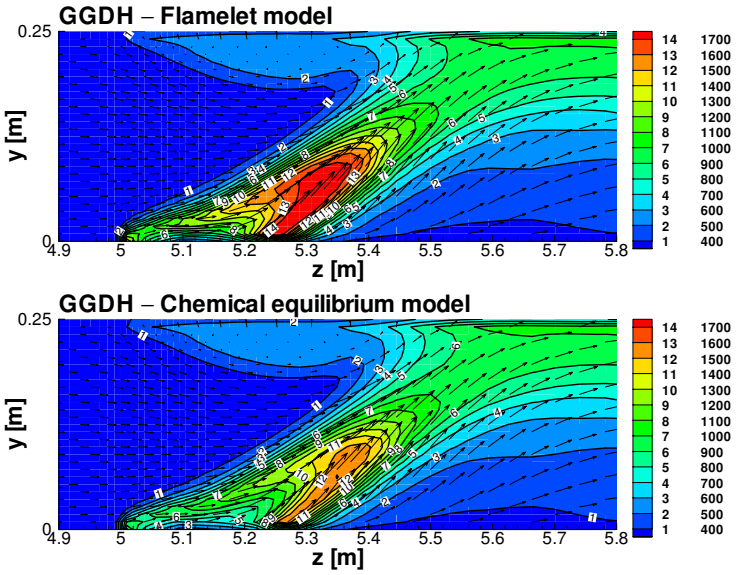

Figure 2. Temperature contours and velocity vectors in the symmetry plane (tunnel B) at critical ventilation velocity. Comparison of the 2 chemistry models (SLFM and FCE).

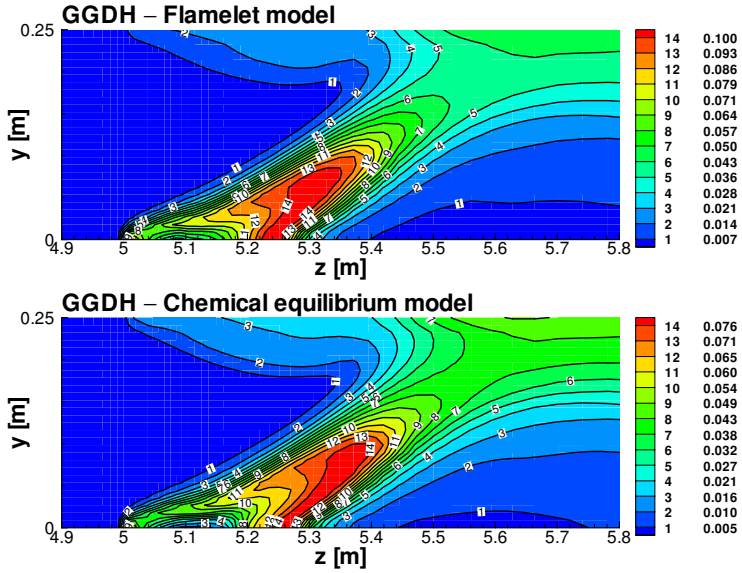

Figure 3. Contour plots of mass-fraction CO_2 (tunnel B).

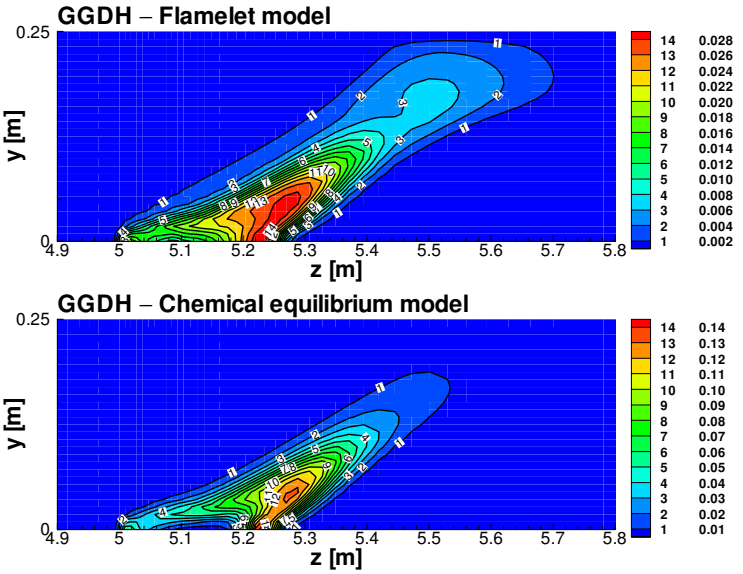

Figure 4. Contour plots of mass-fraction CO (tunnel B).

In order to assess the influence of the cross-sectional geometry, simulation results of the 15 kW fire in tunnel C are given in Figure 5. The measured and predicted critical velocities are given in Table 1. The experimental critical ventilation velocity for this case was also 0.6 m/s. Both variants of the realisable k-ε model are again applied and the results are presented for the numerically determined ventilation velocity. The critical velocity obtained with the SGDH variant of the realisable model is 0.57 m/s, which is again lower than the experimental value. For the GGDH approach, the critical ventilation velocity is 0.6 m/s, which is equal to the experimental value. The SGDH results are obtained with the flamelet model for combustion. For the GGDH approach, both chemistry models are compared. Both

combustion models give the same critical ventilation velocity value. As for tunnel B, the temperatures in the flame are lower with the chemical equilibrium model than with the flamelet model. However, since the temperatures in the impingement region are similar, there is no difference in the amount of smoke that travels opposite to the ventilation.

In order to illustrate the 3-dimensionality of the flow-field, temperature contours and velocity vectors are given in Figure 6 for different horizontal planes parallel to the tunnel floor (the plane of symmetry is located at x = 0 m). These results are given for tunnel B (left column) and tunnel C (right column). The GGDH approach is applied at the critical ventilation velocities. Due to the low velocities, the flow can be considered incompressible. The mass added at the burner source is very small compared to the mass of ventilation air entering the tunnel. The combustion of the fuel releases heat in the flow field, resulting in temperature increases and density decreases. Therefore, according to the conservation of mass, the flow has to accelerate downstream of the fire.

The approaching ventilation air is pushed towards the tunnel wall by the flame (thermal blocking effect). Because tunnel C is twice as wide as tunnel B, the influence of the wall is smaller for tunnel C. For tunnel C, the ventilation air has more "space" to go around the flame. As a consequence, the flame in tunnel C is less tilted than the one in tunnel B, making the distance travelled by the gases before impinging on the ceiling larger in tunnel B than in tunnel C. Therefore, the temperatures in the impingement region of tunnel B are lower than those in tunnel C (the gases have more time to cool as they have to travel a longer distance than in tunnel C) and, consequently, the gases have less power, due to the lower buoyancy, to travel against the ventilation air. We also note the existence of a recirculation zone in the zone of smoke reversal (see position y = 20 cm) for both cases.

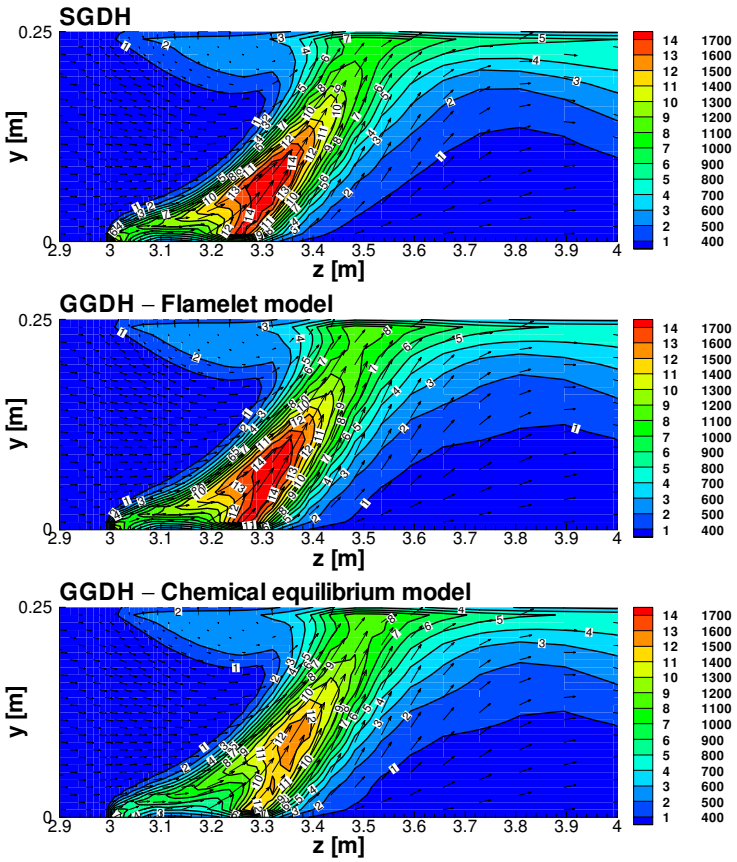

Figure 5. Temperature contours and velocity vectors in the symmetry plane (tunnel C) at critical velocity (SGDH: 0.57 m/s; GGDH: 0.60 m/s).

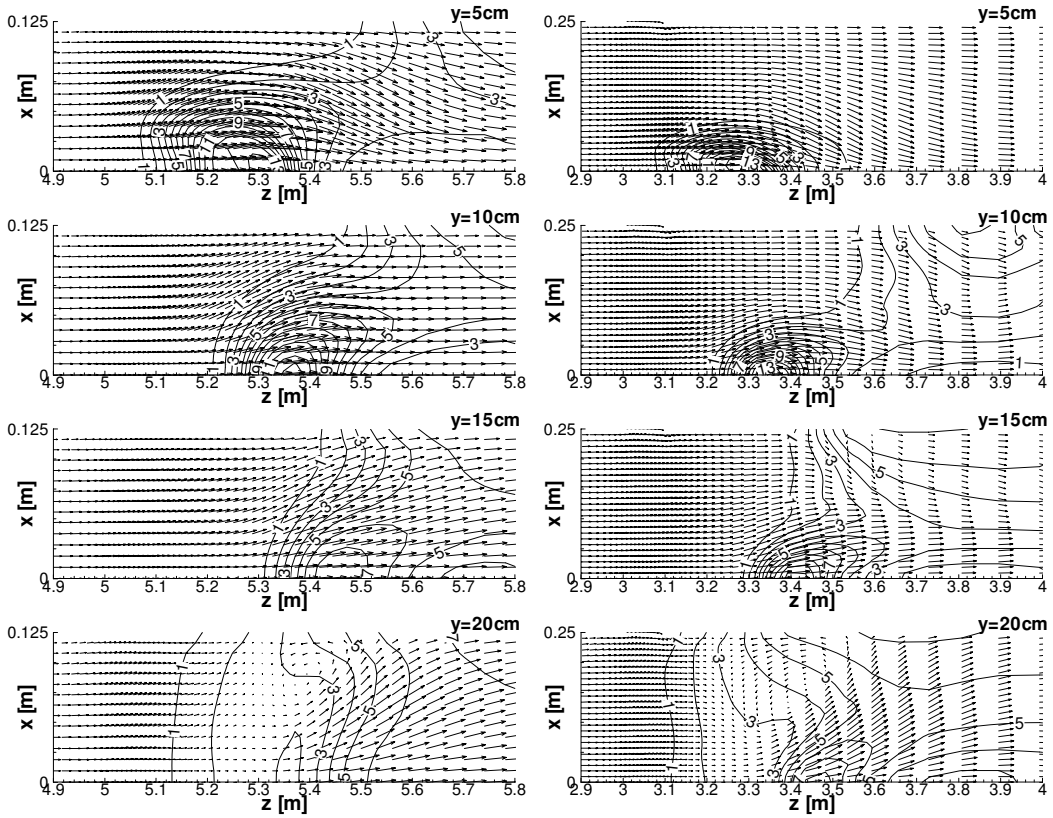

Figure 6. Temperature contours and velocity vectors in horizontal planes parallel to the burner surface. The temperature contours have the same labels as in Figures 1, 2, and 4.

Conclusions

Steady RANS simulations have been performed of a fire in a horizontal, well-ventilated tunnel. The flow-field is complex, due to strong 3-dimensionality. We applied the realisable k-ε model, modified for buoyant flows. Both the simple and the generalised gradient diffusion hypotheses have been used to model the buoyancy source term. The predictions for the critical velocity obtained with the GGDH approach, for both tunnel B and C, are more accurate than the predictions obtained with the SGDH approach.

The global flow fields obtained with both SGDH and GGDH buoyancy source terms are comparable. This is due to the fact that the shear production of turbulent kinetic energy is much more important in this case compared to the effect of buoyancy on turbulence. Still, buoyancy plays an important role in the region where the reversal of the smoke occurs, so that differences between the SGDH approach and the GGDH approach become apparent here.

Two chemistry models have been compared: a steady laminar flamelet model with constant strain and a full chemical equilibrium model. With both models, similar results were obtained; the critical velocity was independent of the chemistry model. With the chemical equilibrium model, lower flame temperatures were observed. Larger differences were observed with respect to CO_2 and (a fortiori) CO mass fraction contours, but no comparison could be made to experimental data.

Overall, the realisable k-ε model combined with the buoyancy term based on the generalised gradient diffusion hypothesis yields good results for the complex case of a tunnel fire. Therefore, in our opinion, the realisable k-ε model, in combination with the GGDH approach for the buoyancy source terms, can be a useful turbulence model for steady RANS simulations of fires.

Acknowledgements

The second author is a Postdoctoral Fellow of the Fund of Scientific Research – Flanders (Belgium) (FWO – Vlaanderen). This research has been funded by Ghent University BOF-project 011/013/04.

Nomenclature

G	buoyancy source term in k-equation
g_i	component of gravity vector in ith direction ($g_1 = 0$, g_2 = -9.81 m/s^2, $g_3 = 0$)
k	turbulent kinetic energy
$S_{\varepsilon B}$	buoyancy source term in ε-equation
u_i	component of velocity vector in ith direction
U_{in}	ventilation velocity
x	x-direction (along the width of the tunnel, positive from symmetry-plane to wall)
y	y-direction (the vertical direction, pointing upwards)
z	z-direction (along the length of the tunnel, positive from tunnel inlet to outlet)
ρ	density
ε	turbulent dissipation rate

Subscripts

$\bar{\phi}$	Reynolds averaged quantity
ϕ'	fluctuation (Reynolds statistics)
$\tilde{\phi}$	Favre averaged quantity
ϕ''	fluctuation (Favre statistics)

References

Brescianini, C.P. and Delichatsios, M.A., "New Evaluation of the k-ε Turbulence Model for Free Buoyant Plumes", Numerical Heat Transfer Part A – Applications, 43, 731-751, 2003.

Correa, S.M., "Turbulence-Chemistry Interactions in the Intermediate Regime of Premixed Combustion", Combustion and Flame, 93, 41-60, 1993.

Daly, B.J. and Harlow, F.H., "Transport Equations in Turbulence", Physics of Fluids, 13, 2634-2649, 1970.

Ince, N.Z. and Launder, B.E., "On the Computation of Buoyancy-Driven Turbulent Flows in Rectangular Enclosures", International Journal of Heat and Fluid Flow, 10, 110-117, 1989.

Merci , B. and Van Maele, K., "Influence of the Turbulence Model in Numerical Simulations of Fire in a Ventilated Horizontal Tunnel", Proceedings of the European Combustion Meeting 2005, Louvain-la-Neuve, Belgium, paper # 115, 2005.

Novozhilov, V., "Computational Fluid Dynamics Modeling of Compartment Fires", Progress in Energy and Combustion Sciences, 27, 611-666, 2001.

Shih, T.H., Liou, W.W., Shabbir, A., Yang, Z. and Zhu, J., "A New k-ε Eddy Viscosity Model for High Reynolds Number Turbulent Flows", Computers and Fluids, 24, 227-238, 1995.

Van Maele, K. and Merci, B., "Application of Two Buoyancy-Modified k-ε Turbulence Models to Different Types of Buoyant Plumes", Fire Safety Journal, 41, 122-138, 2006.

Worthy, J., Sanderson, V. and Rubini, P., "Comparison of Modified k-ε Turbulence Models for Buoyant Plumes", Numerical Heat Transfer Part B – Fundamentals, 39, 151-165, 2001.

Wu, Y. and Bakar, M.Z.A., "Control of Smoke Flow in Tunnel Fires Using Longitudinal Ventilation Systems – A Study of the Critical Velocity", Fire Safety Journal, 35, 363-390, 2000.

Yan, Z. and Holmstedt, G., "A Two-Equation Turbulence Model and Its Application to a Buoyant Diffusion Flame", International Journal of Heat and Mass Transfer, 42, 1305-1315, 1999.

Merci, B., Dick, E., Vierendeels, J. and De Langhe, C., "Determination of ε at inlet boundaries", International Journal of Numerical Methods for Heat & Fluid Flow, 12, 65-80, 2002.